

## Research Paper

# Body City Car Design of Two Passengers Capacity: A Numerical Simulation Study

Randi Purnama Putra<sup>1,2</sup>✉, Dori Yuvenda<sup>1,2</sup>, Muji Setiyo<sup>3,4</sup>, Andrizal<sup>1</sup>, Martias<sup>1</sup>

<sup>1</sup>Department of Automotive Engineering, Universitas Negeri Padang, 25131, Indonesia

<sup>2</sup>Centre For Energy and Power Electronics Research (CEPER), Universitas Negeri Padang, Indonesia

<sup>3</sup>Department of Automotive Engineering, Universitas Muhammadiyah Magelang, 56126, Indonesia

<sup>4</sup>Center of Energy for Society and Industry (CESI), Universitas Muhammadiyah Magelang, Indonesia

✉ randipurnama@ft.unp.ac.id

<https://doi.org/10.31603/ae.6304>



Published by Automotive Laboratory of Universitas Muhammadiyah Magelang collaboration with Association of Indonesian Vocational Educators (AIVE)

## Abstract

### Article Info

Submitted:

30/11/2021

Revised:

01/01/2022

Accepted:

04/01/2022

Online first:

18/04/2022

A city car is needed to overcome congestion and parking spaces in urban areas. However, currently, the body design of the city car is still experiencing problems, namely the value of the large drag coefficient, which causes an increase in fuel consumption. This study aims to design a city car body with two passengers that is more aerodynamic so as to minimize fuel use. This research method is a numerical simulation model using the ANSYS fluent students version 2021. Parameters in the form of drag coefficient values, velocity streamlines and velocity contours on the city car are aerodynamic aspects that are analyzed. The results show that the dimensions of the designed city car have a length of 2.59 m, a width of 1.6 m, and a height of 1.52 m by considering the ergonomic parameters and comfort of the user so that it fits the character of the people in Indonesia. In addition, from the independence grid analysis performed, the value of the number of meshes that have the smallest error value is obtained, namely mesh C (the number of meshes is 129,635). Mesh C has an error of 7.2%. It was found that as the velocity increases, the value of the drag coefficient ( $C_D$ ) produced is relatively smaller. In a city car with a velocity of 10 m/s, the drag coefficient value is 0.599, at a velocity of 20 m/s, the drag coefficient value is 0.594, and a velocity of 30 m/s is a drag coefficient value of 0.591.

**Keywords:** City car; Velocity contours; Velocity streamlines; Drag coefficient

## 1. Introduction

Nowadays, the number of motorized vehicle users is increasing every year, especially in commercial and passenger vehicles [1]. This has an impact on traffic congestion due to the increasing number of vehicles while the road conditions are getting narrower due to the influence of the construction of housing and office buildings, especially in urban areas [2], [3]. Likewise, the increase in the number of vehicles allows the use of more parking areas while the availability of parking areas is currently very limited in urban areas, so that many drivers park their vehicles on the side of the road, resulting in traffic jams [4]. Then also, with the increase in vehicles operating on the road, it is required to be

able to provide traffic safety in order to avoid accidents [5].

In overcoming these problems, one of the efforts made by the automotive industry is to launch a mini car called the future car project, which is termed a city car. Several world manufacturers such as Arcimoto in the United States (US), Smart ForTwo in Germany, Toyota i-TRIL in Japan, and Wuling E100 in China continue to develop future cars with a small size so that it does not bother users [6].

However, with the existence of a city car, it still causes a large drag coefficient, so that it has an impact on increasing fuel consumption [7]–[9]. Mariani et al. [8] explained that a decrease in the coefficient drag could reduce fuel consumption.



This work is licensed under a Creative Commons Attribution-NonCommercial 4.0 International License.

Nasir et al. [10] explained that the coefficient drag could cause an increase in fuel consumption of approximately 6%. Saleh and Ali [11] stated that lowering drag can reduce fuel consumption. Huminic et al. [12] explained that the decrease in drag and lift had a significant impact on fuel consumption. Ashik et al. [13] explained that the 50% increase in fuel consumption was contributed by aerodynamic drag forces.

Several previous studies carried out the design of the vehicle body as done by Sivaraj, G. et al. [14] conducted research by making vehicle body designs by varying the shape of the vehicle's rear body with experimental methods. The results showed that the rear body shape with hatchback and square back models had a better aerodynamic performance. Ashik et al. [13] conducted research by designing the rear body of the vehicle with variations of special tapered and diffuser. The results showed that the diffuser model on the rear body produces a lower drag coefficient of 0.29.

Based on previous research that has been explained, it shows that the design shape and dimensions of the vehicle body affect the drag coefficient on the aerodynamics of the vehicle. This study aims to design a minimalist vehicle body with the concept of a city car with two passengers. The novelty of this research is to

combine the square back model on the rear body with a compact model on the front body of the vehicle with smaller vehicle dimensions so as to produce a lower drag coefficient, thereby reducing fuel consumption. This is a differentiator from previous studies. This study uses a numerical simulation method using the ANSYS fluent students version 2021 software and then analyzes the drag coefficient parameters, velocity contours, and velocity streamline.

## 2. Method

### 2.1. Numerical Setup

The goal of this research is to develop the body of a two-passenger city automobile. The research was carried out utilizing numerical simulations with the Ansys student version 2021 R2 computational fluid dynamics (CFD) program during the design phase. In general, there are two steps to the work in this study: pre-processing and post-processing. The dimensions of the designed city car had a length of 2.59 m, a width of 1.6 m, and a height of 1.52 m (Table 1). The selection of these dimensions has taken into account the ergonomic parameters and comfort of the user. Figure 1 shows a three-dimensional representation of a city automobile with two passengers.

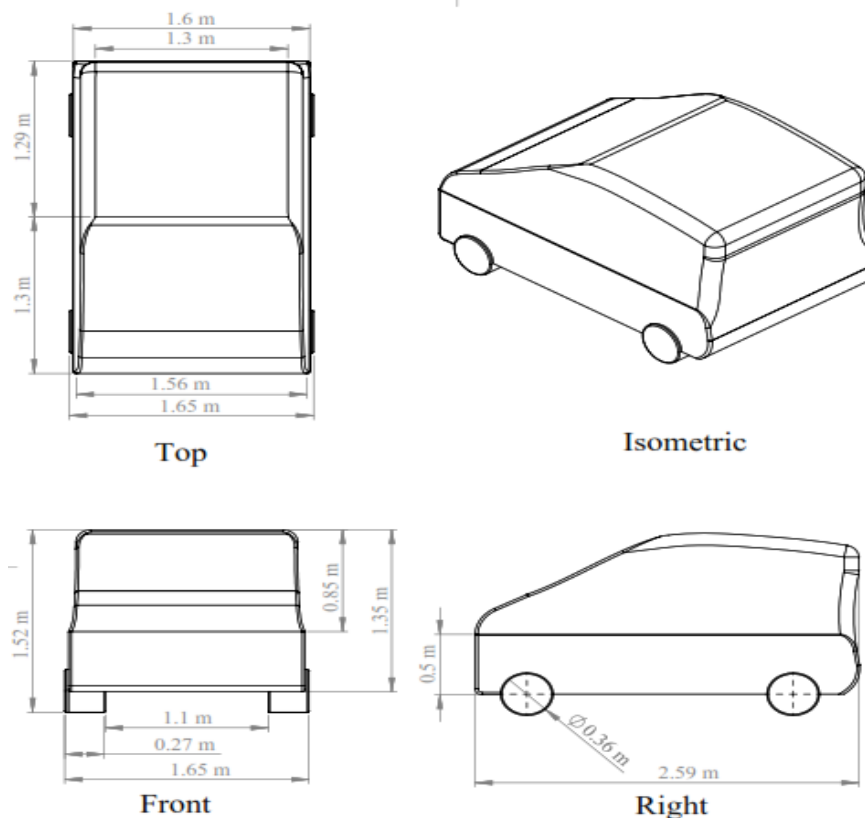


Figure 1. Body design of a city car with two passengers

**Table 1.** The dimensions of city car

Name	Dimensions (m)
Length	2.59
Width	1.6
Height	1.52

In this study, the order of work includes creating geometry, meshing, determining the boundary type, deciding the solver, and analyzing the outcomes. Solidworks software creates geometry by generating a set of available coordinates and edges. The type of poly hexacore mesh is employed for the meshing volume. The meshing technique was adopted as a grading system with progressively dense mesh distribution on all sides surrounding the city car's body design. The fluid material characteristics are air at temperature ( $T$ ) = 28 °C, density ( $\rho$ ) = 1.172 kg/m<sup>3</sup>, and absolute viscosity ( $\mu$ ) = 1.8586 × 10<sup>-5</sup> N.s/m<sup>2</sup>. This study's solution employs the SIMPLE technique and second-order discretization for pressure, second-order upwind for momentum, turbulence kinetic energy, and turbulence

dissipation rate. The convergence criteria for continuity, x-velocity, y-velocity, and z-velocity are established at 10<sup>-6</sup> in the iteration process. The inlet region is specified by a velocity of 10, 20, and 30 m/s and a turbulence intensity of 5% under boundary circumstances (Table 2). Figure 2 shows a detailed picture from the top perspective to help illustrate the meshing that has been done.

**2.2. Turbulence Model**

The most widely used turbulence model in computational fluid dynamics is the K-epsilon ( $k-\epsilon$ ) model. This turbulence model represents average flow properties in turbulent flow scenarios. The K-epsilon model tries to improve the "mixing-length model" in moderate to high flow complexity by algebraically specifying the turbulent length scale. Turbulent kinetic energy is the first variable that explains the energy in turbulence ( $k$ ). The second variable, turbulent dissipation, describes the rate of dissipation of turbulent kinetic energy (epsilon).

**Table 2.** Boundary Condition Settings

Name	Boundary Type	Boundary Details
Inlet	Velocity Inlet	1. Magnitude (measured normal to Boundary): 10, 20, and 30 m/s 2. Turbulence: medium (intensity = 5%)
Outlet	Pressure Outlet	1. Gauge Pressure magnitude: normal to boundary 2. Intensity and Viscosity Ratio for turbulence methods
Symmetry	Symmetry	
Car body	Wall	1. Mass and momentum: no-slip wall 2. Wall Roughness: smooth wall
Top	Wall	Mass and momentum: specified shear
Bottom	Wall	1. Mass and momentum: slip wall 2. Wall Roughness: smooth wall
Left	Wall	Mass and momentum: specified shear

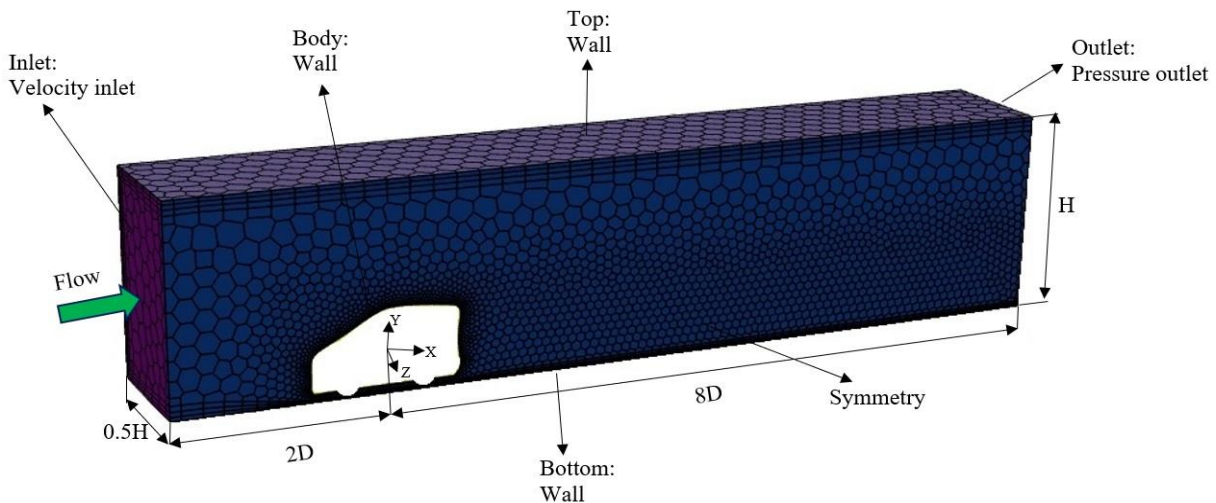


**Figure 2.** Numerical setup

The  $k$ - RNG,  $k$ -standard and  $k$ -Realizable turbulence models make up the K-epsilon turbulence model. The semi-empirical  $k$ -standard model is based on the turbulence kinetic energy ( $k$ ) and dissipation rate ( $\epsilon$ ) equations from the transport model. This model includes two transport equations to turbulence, the first of which is turbulent kinetic energy ( $k$ ) and the second of which is turbulence dissipation ( $\epsilon$ ). The quantity of energy in the turbulence is represented by the value of  $k$ , while the size of the turbulence is represented by the value. A three-dimensional (3-D) flow simulation technique with a high level of precision is used to get accurate and reliable results in a computational manner. This is a fully functional semi-empirical turbulence model. The transport equation yields the turbulent kinetic energy ( $k$ ) and its dissipation rate ( $\epsilon$ ) as follows Eq. (1) and (2):

The average velocity gradient generates turbulent kinetic energy, which is represented by  $G_k$  in this equation.  $C_{1\epsilon}$  is a constant,  $C_{2\epsilon}$  is a constant, and  $C_{3\epsilon}$  is a constant. For  $k$  and  $\epsilon$  are turbulent Prandtl numbers. The turbulent viscosity, often known as eddy ( $\mu_t$ ), is determined by multiplying  $k$  and  $\epsilon$  (Eq. 3).

### 2.3. Grid Independency Analysis

Grid independency analysis is needed to determine the optimal number of mesh used in running CFD and has the smallest error. The evaluation of the number of meshes used is 106,747, 118,840, 129,635, and 142,726. In order to facilitate the naming of each of these meshes, the meshes are named A, B, C, and D. Mesh A has a mesh count of 106,747, mesh B has a mesh count of 118,840, mesh C has a mesh count of 129,635, and mesh D has a mesh count of 142,726. **Table 3**

$$\frac{\partial}{\partial t}(\rho k) + \frac{\partial}{\partial x_i}(\rho k u_i) = \frac{\partial}{\partial x_j} \left[ \left( \mu + \frac{\mu_t}{\sigma_k} \right) \frac{\partial k}{\partial x_j} \right] + G_k - \rho \epsilon \tag{1}$$

$$\frac{\partial}{\partial t}(\rho \epsilon) + \frac{\partial}{\partial x_i}(\rho \epsilon u_i) = \frac{\partial}{\partial x_j} \left[ \left( \mu + \frac{\mu_t}{\sigma_\epsilon} \right) \frac{\partial \epsilon}{\partial x_j} \right] + C_{1\epsilon} \frac{\delta}{k} (G_k + C_{3\epsilon} G_b) - C_{2\epsilon} \rho \frac{\delta^2}{k} + S_\epsilon \tag{2}$$

$$\mu_t = \rho C_\mu \frac{k^2}{\delta} \tag{3}$$

where  $C_\mu$  denotes a constant [16]

$$C_D = \frac{2F_D}{\rho u^2 A} \tag{4}$$

shows the results of grid independency study for various meshing. The drag coefficient on a city automobile with a velocity ( $V$ ) of 10 m/s is used to examine grid independence. The drag coefficient ( $C_D$ ) is a dimensional quantity used to measure the resistance or resistance of an object in a fluid environment such as air. Eq. (4) expresses the drag coefficient.

From the grid independency analysis performed, the value of the mesh that has the smallest error value is meshing C. Mesh C has a 7.2 percent error, defined as the difference between the  $C_D$  of the reference mesh and the  $C_D$  of the experiment divided by the  $C_D$  of the experiment (% error = [(( $C_D$  of the reference mesh) - ( $C_D$  of the experiment)) / ( $C_D$  of the experiment)] x 100%. Furthermore, this mesh C is used to evaluate the flow characteristics of the city car. The validation of the results of the numerical research was carried out by comparing the  $C_D$  of several meshes (A, B, C, D) to the  $C_D$  of the experimental results, as shown in **Figure 3**.

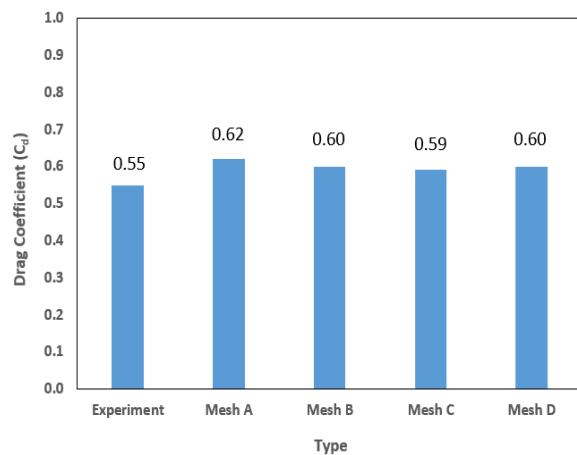


**Figure 3.** Comparison of the  $C_D$  value in each mesh with the  $C_D$  of the experiment [15]

**Table 3.** Grid Independence Analysis

Mesh Type	Number of Mesh (Cells)	Drag Coefficient ( $C_D$ )	Error (%)
Experiment	-	0.55	-
Mesh A	106,747	0.62	12.7
Mesh B	118,840	0.60	9.0
Mesh C	129,635	0.59	7.2
Mesh D	142,726	0.60	9.0

### 3. Result and Discussion

This study aims to design a city car body with a capacity of two passengers. The design concept of a city car that is carried out in this study is to combine a compact shape on the front and a square back on the back of the city car body (Figure 4). This is intended so that the appearance of the city car is more sporty, minimalist, more aerodynamic, and can be used for everyday purposes. The minimalist design and body size of the city car is expected to be used by consumers in urban areas. The city car body design process starts from literature review, making designs, and testing aerodynamics. To provide an in-depth analysis technique regarding the design of a city car body on aerodynamic effects, it is necessary to conduct a discussion on the results of the evaluation of this study which is supported by several other studies. In this chapter, the result data is presented in the form of graphs and their explanations. It consists of a graph of the drag coefficient ( $C_D$ ), as well as a velocity contour. The drag coefficient data ( $C_D$ ) was obtained at the velocity of 10 m/s, 20 m/s, and 30 m/s.

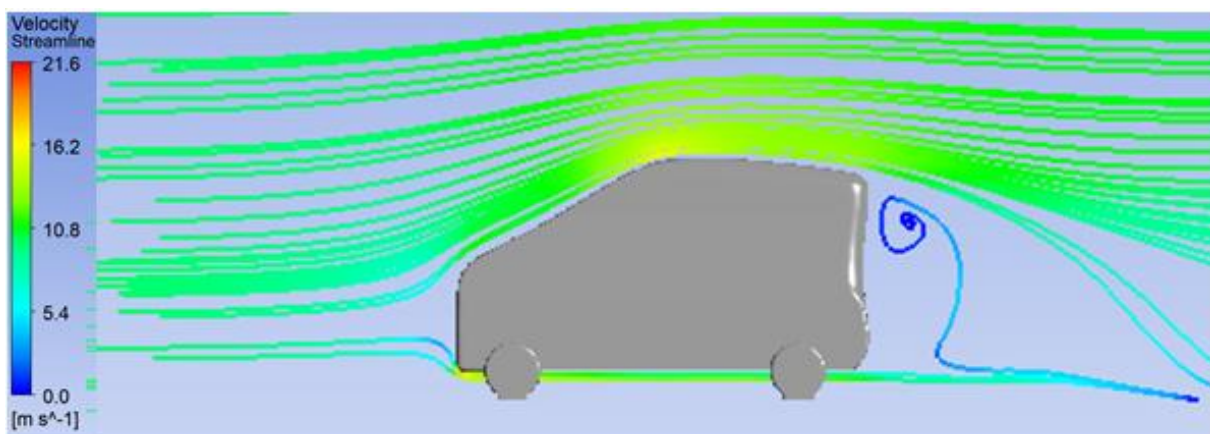
#### 3.1. Drag Coefficient ( $C_D$ )

The results show that the dimensions of the designed city car have a length of 2.59 m, a width

of 1.6 m, and a height of 1.52 m (Figure 1). The shape of the city car design has been designed as a compact shape on the front. This results in a separated flow from the city car and forms a smaller separation vortex. The presence of a small separation vortex will produce a low-pressure area behind the body called the wake, which is also small (Figure 6). This greatly contributes to the reduction of the drag coefficient ( $C_D$ ) of the body. The reduction in the value of the drag coefficient has a correlation with the reduction in fuel use in the city car (Xingjun et al. [17]). Figure 5 shows the drag coefficient data at velocity of 10 m/s, 20 m/s, and 30 m/s. The figure shows that with increasing velocity, the value of the drag coefficient ( $C_D$ ) produced is relatively smaller. In a city car with a velocity of 10 m/s, the drag coefficient value is 0.599, a velocity of 20 m/s gets a drag coefficient value of 0.594, and a velocity of 30 m/s gets a drag coefficient value of 0.591.

#### 3.2. Velocity Contour and Velocity Streamline

Figure 6 shows the velocity contours of a city car with a velocity of 10 m/s, 20 m/s, and 30 m/s. The picture shows that the velocity contour on the back of the city car body has a low velocity, both at a velocity of 10 m/s, 20 m/s, and 30 m/s. This slow velocity is shown in blue in the figure. This

**Figure 4.** Velocity streamlines on the city car

indicates that on the back of the city car body, a vortex or wake is formed. For more details, in [Figure 7](#) you can see the velocity streamline on the side of the city car body. Velocity streamline are taken at a velocity of 10, 20, and 30 m/s. In [Figure 6](#), it can be seen that the flow is separated on the rear contour of the body of the city car and moves downwards. This downward flow is what eventually forms a wake behind the city car body. At a velocity of 20 and 30 m/s, it can be seen that the wake formed behind the body of the city car is smaller than the velocity of 10 m/s.

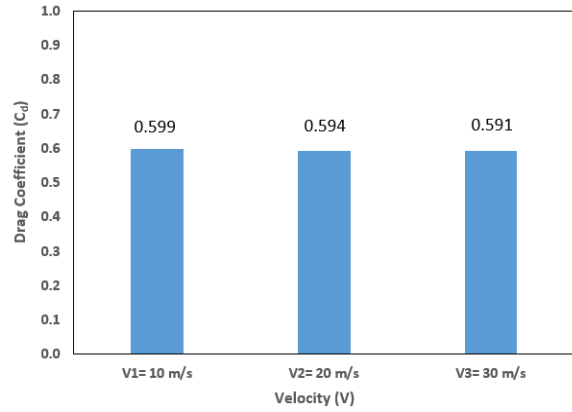


**Figure 5.** Comparison of  $C_d$  values at velocity of 10 m/s, 20 m/s and 30 m/s

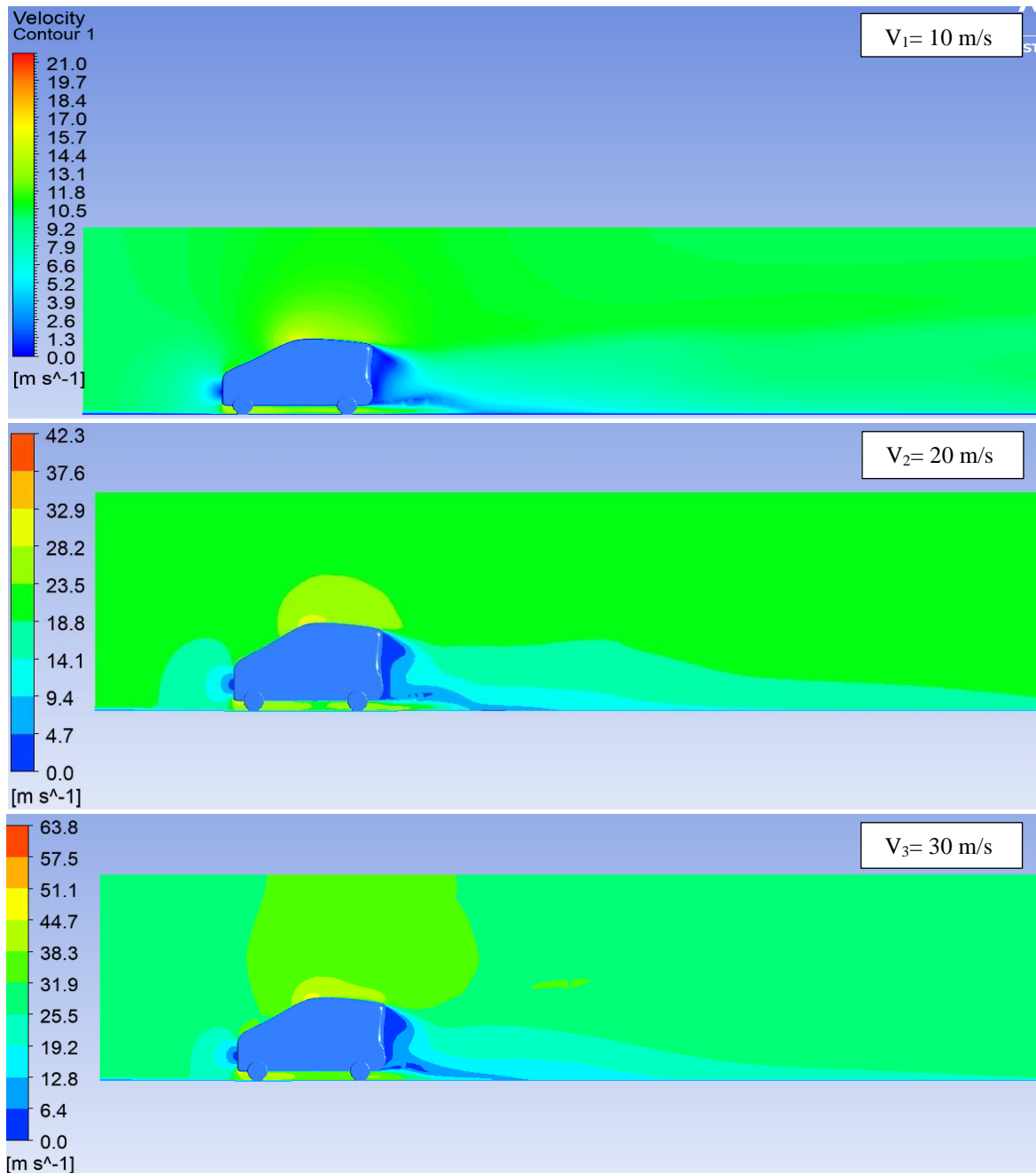


**Figure 6.** Velocity contour at a velocity of 10, 20, and 30 m/s

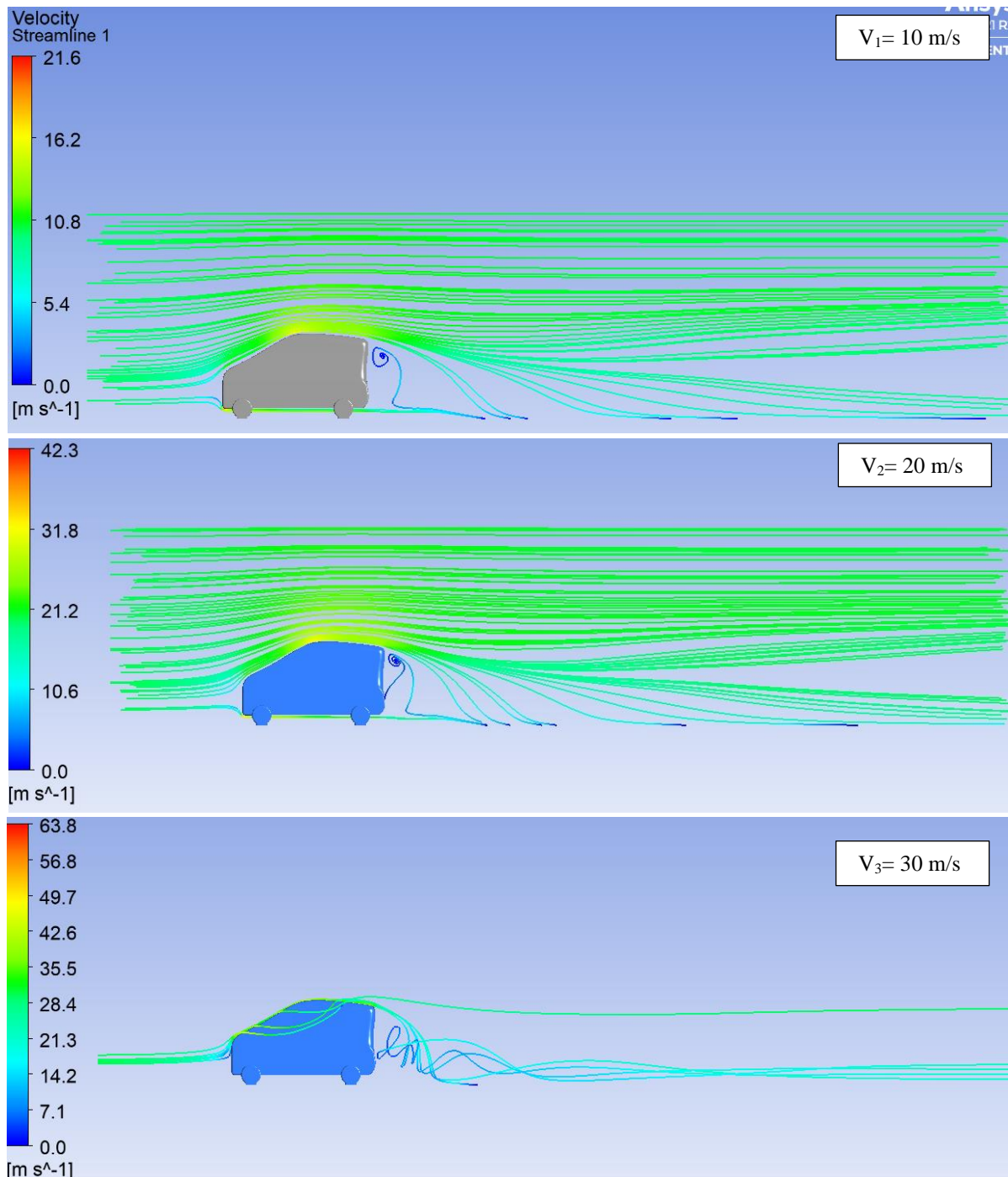


Figure 7. Velocity streamlines at a velocity of 10, 20, and 30 m/s

### 3.3. Velocity Streamline in the Top View of Body Car

The shape of the square back on the back of the city car body also has an impact on the improvement of the characteristics of the  $C_D$ . This is contributed by the body shape of the back of the curved city car. Several studies also concluded the effect of body shape on the body's  $C_D$  value, such as research conducted by Xingjun et al. [17]. The square back shape on the back of the city car body can control the separation of the flow boundary

layer under the car and avoid the turbulence phenomenon behind it (Figure 8). Humnic et al. [18] also experimentally investigated the effect of the diffuser on the rear of the car body and revealed better performance by using a curved-type diffuser. Similarly, Rossitto et al. [19] investigated the afterbody rounding in the upper body and the effect of the diffuser, Kekus and Angland [20] investigated the Ahmed-type body, and Ehirim et al. [21] studied the underbody diffuser, which has a convex protrusion,

Grandemange et al. [22] and Bonnavion and Cadot [23] also analyzed the effect of the underbody diffuser in the shape of a boat tail on the aerodynamics of the Ahmed-type body.

Figure 8 shows velocity streamlines at the top of the city car body. Velocity streamline are taken at a velocity of 10, 20, and 30 m/s. In the figure, it can be seen that the flow is separated on the back contour of the body of the city car and forms a separation vortex. The chronology of the 3D separation vortex begins when the flow under the vehicle flows into the side body and then interacts with the flow in the side body, which has a fairly complex contour change, which ultimately results in a 3D separation vortex. This phenomenon occurs at all velocities of 10, 20, and 30 m/s.

#### 4. Conclusion

This study aims to design a city car body with two passengers that is more aerodynamic so as to minimize fuel use. This research method is a numerical simulation model using the ANSYS Fluent students version 2021. From the grid independence analysis performed, the value of the mesh that has the smallest error value is meshing C. Mesh C has a 7.2 percent error,

defined as the difference between the  $C_D$  of the reference mesh and the  $C_D$  of the experiment. The results showed that the dimensions of the designed city car had a length of 2.59 m, a width of 1.6 m, and a height of 1.52 m. The selection of these dimensions has taken into account the ergonomic parameters and comfort of the user. So it is hoped that the selection of these dimensions is suitable for the character of the people in Indonesia. In addition, information is obtained that with increasing velocity, the value of the drag coefficient ( $C_D$ ) produced is relatively smaller. In a city car with a velocity of 10 m/s, the drag coefficient value is 0.599, a velocity of 20 m/s gets a drag coefficient value of 0.594, and a velocity of 30 m/s gets a drag coefficient value of 0.591. Further research will determine the mechanism of vehicle motion and body city car refinement for future work.

#### Acknowledgement

The researcher expresses high appreciation and thanks to the Research and Community Service Institute, Universitas Negeri Padang for funding this research with a research contract number: 695/UN35.13/LT/2021.

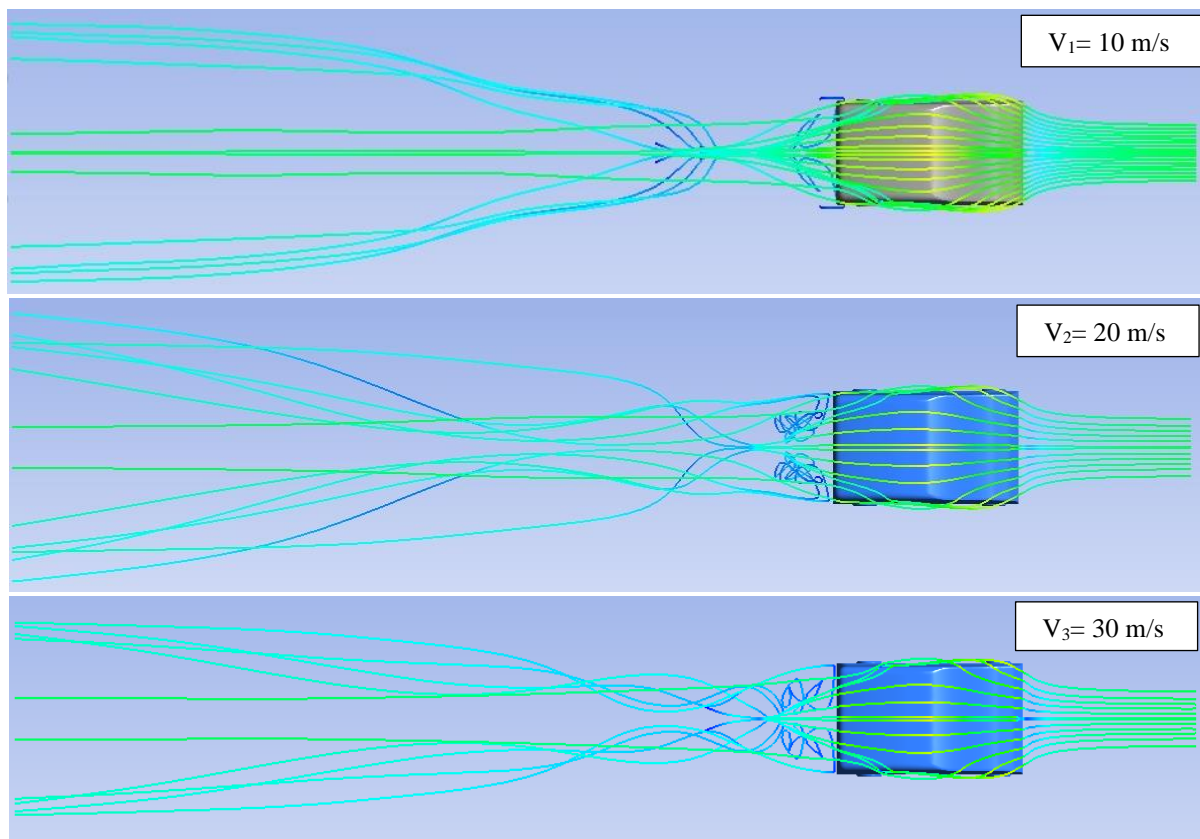


Figure 8. Velocity streamline at a velocity of 10, 20, and 30 m/s (top view)

## Author's Declaration

### Authors' contributions and responsibilities

The authors made substantial contributions to the conception and design of the study. The authors took responsibility for data analysis, interpretation and discussion of results. The authors read and approved the final manuscript.

### Funding

This research funded by Universitas Negeri Padang with a research contract number: 695/UN35.13/LT/2021.

### Availability of data and materials

All data are available from the authors.

### Competing interests

The authors declare no competing interest.

### Additional information

No additional information from the authors.

## References

- [1] UK Department for transport, "Road Use Statistics GB 2016," *JPEN. Journal of parenteral and enteral nutrition*, vol. 3, no. 6, pp. 452–6, 2016.
- [2] Public Works and Housing Ministry, "Indonesian Infrastructure Statistics," *Pusdatin*, vol. 53, no. 9, pp. 1–58, 2020.
- [3] S. Selzer and M. Lanzendorf, "On the road to sustainable urban and transport development in the automobile society? Traced narratives of car-reduced neighborhoods," *Sustainability (Switzerland)*, vol. 11, no. 16, 2019, doi: 10.3390/su11164375.
- [4] D. Shoup, *Parking and the City*, no. July. 2018.
- [5] D. W. Karmiadji, M. Gozali, M. Setiyo, T. Raja, and T. A. Purnomo, "Comprehensive Analysis of Minibuses Gravity Center: A Post-Production Review for Car Body Industry," *Mechanical Engineering for Society and Industry*, vol. 1, no. 1, pp. 31–40, 2021, doi: 10.31603/mesi.5250.
- [6] A. Gussmann, "Analysis of the applicability of a mobility concept without private cars for the Maun Science Park Botswana," 2010.
- [7] A. Ekoprianto, "Analisis Aerodinamika Pada Mobil Listrik Type Citycar Untuk Lingkungan Kampus," *Jurnal Konversi Energi dan Manufaktur*, vol. 3, pp. 125–130, 2016.
- [8] F. Mariani, C. Poggiani, F. Risi, and L. Scappaticci, "Formula-SAE racing car: Experimental and numerical analysis of the external aerodynamics," *Energy Procedia*, vol. 81, pp. 1013–1029, 2015, doi: 10.1016/j.egypro.2015.12.111.
- [9] A. Yudianto, I. W. Adiyasa, and A. Yudianto, "Aerodynamics of Bus Platooning under Crosswind," *Automotive Experiences*, vol. 4, no. 3, pp. 119–130, 2021, doi: <https://doi.org/10.31603/ae.5298>.
- [10] R. E. M. Nasir *et al.*, "Aerodynamics of ARTEC's PEC 2011 EMO-C car," *Procedia Engineering*, vol. 41, no. Iris, pp. 1775–1780, 2012, doi: 10.1016/j.proeng.2012.07.382.
- [11] Z. M. Saleh and A. H. Ali, "Numerical Investigation of Drag Reduction Techniques in a Car Model," *IOP Conference Series: Materials Science and Engineering*, vol. 671, no. 1, 2020, doi: 10.1088/1757-899X/671/1/012160.
- [12] A. Humnic and G. Humnic, "Aerodynamics of curved underbody diffusers using CFD," *J. Wind Eng. Ind. Aerodyn.*, vol. 205, p. 104300, 2020, doi: 10.1016/j.jweia.2020.104300.
- [13] P. A. Nigal Ashik, P. Suseendhar, N. Manoj, and S. Wasim Feroze, "Reduction of drag in box-type and half streamlined automobile vehicles," *Materials Today: Proceedings*, no. xxxx, 2020, doi: 10.1016/j.matpr.2020.11.109.
- [14] G. Sivaraj, K. M. Parammasivam, M. S. Prasath, P. Vadivelu, and D. Lakshmanan, "Low analysis of rear end body shape of the vehicle for better aerodynamic performance," *Materials Today: Proceedings*, vol. 47, no. xxxx, pp. 2175–2181, 2021, doi: 10.1016/j.matpr.2021.05.521.
- [15] J. Carvill, "4 - Fluid mechanics," J. B. T.-M. E. D. H. Carvill, Ed. Oxford: Butterworth-Heinemann, 1993, pp. 146–171.
- [16] R. P. Putra, Sutardi, and W. A. Widodo, "Experimental and numerical studies of pressure drop reduction in a 90° square elbow with the addition of circular turbulators," *Int. Rev. Mech. Eng.*, vol. 13, no. 10, pp. 608–618, 2019, doi: 10.15866/ireme.v13i10.18148.
- [17] X. Hu, R. Zhang, J. Ye, X. Yan, and Z. Zhao, "Influence of different diffuser angle on Sedan's aerodynamic characteristics," *Physics Procedia*, vol. 22, pp. 239–245, 2011, doi: 10.1016/j.phpro.2011.11.038.
- [18] A. Humnic and G. Humnic, "Aerodynamic Study of A Generic Car Model With Wheels and Underbody Diffuser," *International Journal of Automotive Technology*, vol. 18, no. 3, p. 397–404, 2017.

- [19] G. Rossitto, C. Sicot, V. Ferrand, J. Borée, and F. Harambat, "Aerodynamic performances of rounded fastback vehicle," *Proceedings of the Institution of Mechanical Engineers, Part D: Journal of Automobile Engineering*, vol. 231, no. 9, pp. 1211–1221, 2017, doi: 10.1177/0954407016681684.
- [20] P. Kekus and D. Angland, "Automatic wind tunnel-based optimisation of an automotive underbody diffuser," *AIAA Aerospace Sciences Meeting, 2018*, no. 210059, 2018, doi: 10.2514/6.2018-0045.
- [21] O. H. Ehirim, K. Knowles, and A. J. Saddington, "A review of ground-effect diffuser aerodynamics," *Journal of Fluids Engineering, Transactions of the ASME*, vol. 141, no. 2, pp. 1–19, 2018, doi: 10.1115/1.4040501.
- [22] M. Grandemange *et al.*, "A study of wake effects on the drag of Ahmed's squareback model at the industrial scale," *Journal of Wind Engineering and Industrial Aerodynamics*, vol. 145, pp. 282–291, 2015, doi: 10.1016/j.jweia.2015.03.004.
- [23] G. Bonnavion and O. Cadot, "Boat-tail effects on the global wake dynamics of a flat-backed body with rectangular section," *Journal of Fluids and Structures*, vol. 89, no. 2018, pp. 61–71, 2019, doi: 10.1016/j.jfluidstructs.2019.01.009.